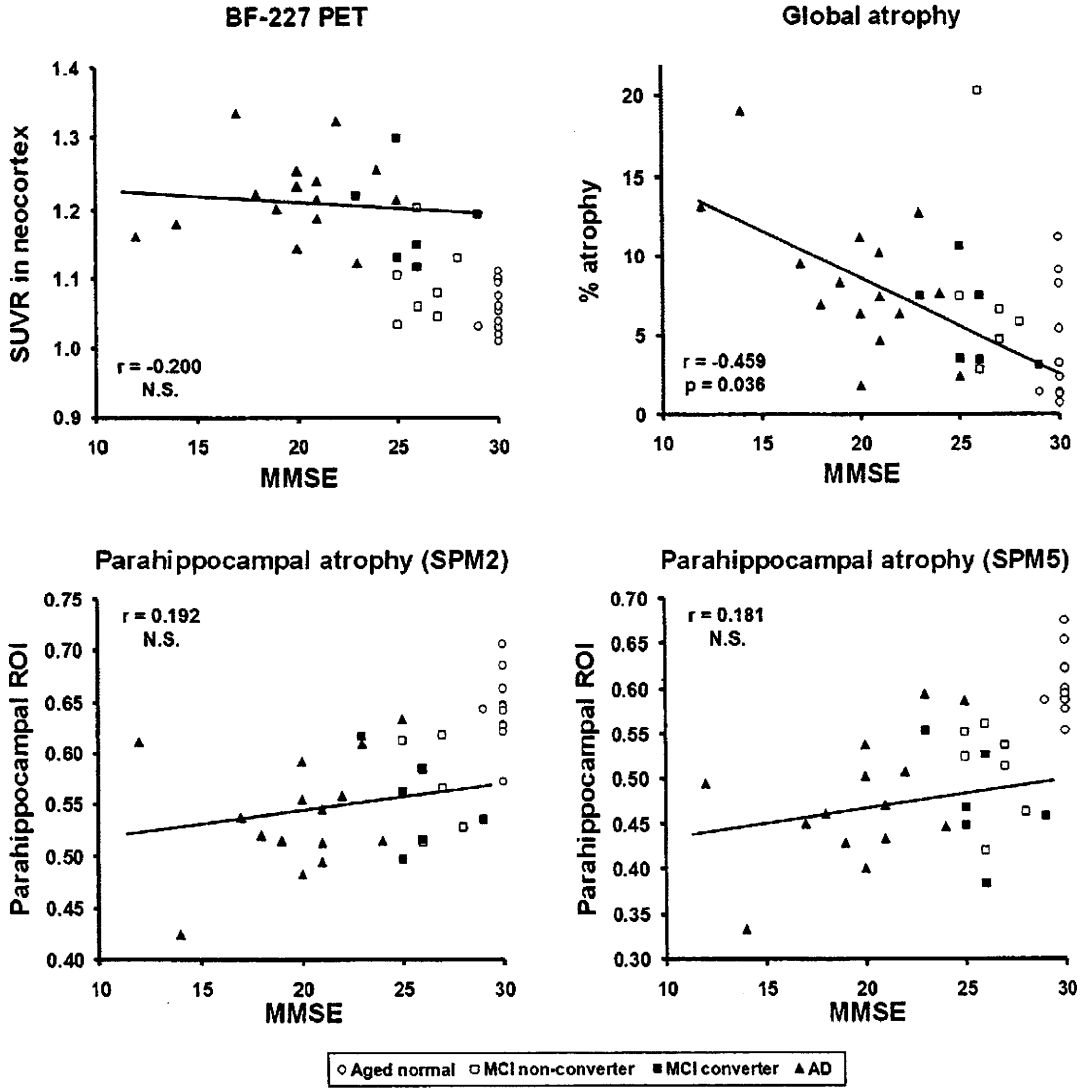

Fig. 6. The correlations of MMSE scores with the BF-227 SUVR in the neocortex (upper left), the percent global atrophy (upper right), the parahippocampal region of interest (ROI) value from gray matter images processed by SPM2 (lower left), and the parahippocampal ROI value from gray matter images processed by SPM5 (lower right). Open circle: control; open square: MCI non-converter; filled square: MCI converter; filled triangle: AD.

binding are proceeding to AD [43]. In our study, almost all normal subjects exhibited a normal distribution of BF-227 in the brain. This finding may suggest a lower sensitivity of diffuse amyloid plaque detection by BF-227 [22]. However, the proportion of amyloid PET-positive individuals in the normal population varies greatly depending on the characteristics of the sample population. Indeed, the mean age of the control subjects in our study was somewhat younger than in previous PIB–PET studies. Therefore, a direct comparison of BF-227–PET with PIB–PET in the same normal population is necessary to compare the ability of these agents to detect early AD pathology. A longitudinal follow-up of amyloid PET-positive cases in the healthy, normal population will also elucidate whether tracer uptake reflects pre-symptomatic detection of AD or a false-positive finding. A follow-up study of the patients with AD using PIB–PET showed that the amyloid deposition remains high but stable, despite decreases in regional glucose metabolism and cognitive function.[44] Our cross-sectional analysis also revealed a plateau of cortical BF-227 uptake in early AD patients, suggesting that amyloid formation reaches a plateau early in the course of AD. A potential limitation of this study is that it used a semiquantitative SUV measure to estimate BF-227 binding to amyloid plaques. The levels of neocortical BF-227 SUV might be underestimated due to hypoperfusion in AD patients. Quantitative analysis should be performed in future analyses to eliminate the influence of blood flow change.

A previous PIB–PET study found a positive correlation between the rate of whole brain atrophy and amyloid plaque load. [45] However, a recent PET study discovered a discrepancy between regional PIB retention and gray matter loss [38]. Additionally, histopathological analysis revealed no association between Aβ burden and brain atrophy [46]. The present study also found no significant correlation between neocortical BF-227 uptake and global gray matter loss in AD patients, in agreement with these findings. In our correlation analysis of the four measurements with the MMSE scores, we confined our analysis to AD patients and MCI converters because these patients share the same pathological process underlying AD. Therefore, this is more appropriate for the correlation analysis between cognitive function and the degree of Aβ burden or cerebral atrophy induced by the pathological process of AD than an analysis using all samples, including the normal population. In this analysis, the global gray matter loss measured by VBM–MRI was better correlated with MMSE scores than was the Aβ burden measured by BF-227–PET. A similar correlation analysis performed using PIB–PET demonstrated that the

magnitudes of the correlations were greater for hippocampal atrophy than for neocortical PIB retention [38]. The current result, showing no significant correlation of the parahippocampal gray matter density with the MMSE score, seems to be inconsistent with previous PIB–PET data. We believe this discrepancy to be due mainly to differences in the sample population. The analysis in the previous PIB–PET study was performed using all the subjects, including the normal controls; our analysis was confined to AD patients and MCI converters who had already developed severe memory decline and probably substantial neuron loss in the hippocampus. These results suggest that global, rather than parahippocampal, gray matter loss is a potent indicator of dementia severity after the onset of memory loss in AD. We hope to explore the relationship between these imaging measurements and the impairment of episodic memory function in a future study.

It has been reported that the degree or rate of change of cerebral atrophy as measured by MRI analysis is closely related to the clinical progression of dementia [29,30]. Karas et al. performed a VBM–MRI analysis to examine the global and regional gray matter loss in normal, MCI and AD subjects, finding a significantly lower global gray matter volume in the AD subjects and an intermediate volume in the MCI subjects [31]. They followed the MCI subjects and observed greater gray matter loss in the MCI converters than in non-converters [37]. Another study also revealed different patterns of gray matter density distribution between MCI converters and non-converters [35]. From these findings, it appears that gray matter loss in VBM is a good indicator of conversion from MCI to AD. We failed to demonstrate significant inter-group differences between the MCI converters and non-converters, although the MCI converters showed a tendency toward lower parahippocampal gray matter density than did the non-converters. This, however, may be due to the small sample size and insufficient follow-up period (over two years) of the MCI subjects in this study. For example, one MCI non-converter in our study showed an abnormality in both the BF-227 SUVR and parahippocampal gray matter density; extending the follow-up period of the MCI subjects would likely result in more consistent correlation between MCI conversion to AD and the described measurements. Additional longitudinal studies are also needed to confirm the findings we have obtained and to examine the time course of AD, including changes in the pre-symptomatic subjects, and to determine the relationship between amyloid deposition and brain atrophy as underlying factors in the pathogenesis of AD.

Acknowledgements

We appreciate the technical assistance of Dr. S. Watanuki, Dr. Y. Ishikawa, Dr. M. Mori, and Dr. K. Sugi in the clinical PET studies and the support of Fukushimura Hospital for the histochemical studies. We also thank to Dr. H. Akatsu and Dr. T. Yamamoto for supplying brain samples. This study was supported by the Program for the Promotion of Fundamental Studies in Health Science of the National Institute of Biomedical Innovation, the Industrial Technology Research Grant Program in 2004 of the New Energy and Industrial Technology Development Organization (NEDO) of Japan, Health and Labor Sciences Research Grants for Translational Research from the Ministry of Health, an Asan Trazeneca Research Grant, and the Novartis Foundation for Gerontological Research.

References

[1] Blennow K, de Leon MJ, Zetterberg H. Alzheimer's disease. Lancet 2006;368: 387–403.
[2] Drachman DA. Aging of the brain, entropy, and Alzheimer disease. Neurology 2006;67:1340–52.
[3] Braak H, Braak E. Neuropathological stageing of Alzheimer-related changes. Acta Neuropathol 1991;82:239–59.
[4] Arnold SE, Hyman BT, Flory J, Damasio AR, Van Hoesen GW. The topographical and neuroanatomical distribution of neurofibrillary tangles and neuritic plaques in the cerebral cortex of patients with Alzheimer's disease. Cereb Cortex 1991;1:103–16.
[5] Mouton PR, Martin LJ, Calhoun ME, Dal Forno G, Price DL. Cognitive decline strongly correlates with cortical atrophy in Alzheimer's dementia. Neurobiol Aging 1998;19:371–7.
[6] Masters CL, Cappai R, Barnham KJ, Villemagne VL. Molecular mechanisms for Alzheimer's disease: implications for neuroimaging and therapeutics. J Neurochem 2006;97:1700–25.
[7] Nordberg A. PET imaging of amyloid in Alzheimer's disease. Lancet Neurol 2004;3: 519–27.
[8] Villemagne VL, Rowe CC, Macfarlane S, Novakovic KE, Masters CL. Imaginem oblivionis: the prospects of neuroimaging for early detection of Alzheimer's disease. J Clin Neurosci 2005;12:221–30.
[9] Mathis CA, Klunk WE, Price JC, DeKosky ST. Imaging technology for neurodegenerative diseases: progress toward detection of specific pathologies. Arch Neurol 2005;62:196–200.
[10] Nordberg A. Amyloid imaging in Alzheimer's disease. Curr Opin Neurol 2007;20: 398–402.
[11] Small GW, Kepe V, Ercoli LM, Siddarth P, Bookheimer SY, Miller KJ, et al. PET of brain amyloid and tau in mild cognitive impairment. N Engl J Med 2006;355:2652–63.
[12] Klunk WE, Engler H, Nordberg A, Wang Y, Blomqvist G, Holt DP, et al. Imaging brain amyloid in Alzheimer's disease with Pittsburgh Compound-B. Ann Neurol 2004;55:306–19.
[13] Price JC, Klunk WE, Lopresti BJ, Lu X, Hoge JA, Ziolko SK, et al. Kinetic modeling of amyloid binding in humans using PET imaging and Pittsburgh Compound-B. J Cereb Blood Flow Metab 2005;25:1528–47.
[14] Lopresti BJ, Klunk WE, Mathis CA, Hoge JA, Ziolko SK, Lu X, et al. Simplified quantification of Pittsburgh Compound B amyloid imaging PET studies: a comparative analysis. J Nucl Med 2005;46:1959–72.
[15] Rowe CC, Ng S, Ackermann U, Gong SJ, Pike K, Savage G, et al. Imaging beta-amyloid burden in aging and dementia. Neurology 2007;68:1718–25.
[16] Mintun MA, Larossa GN, Sheline YI, Dence CS, Lee SY, Mach RH, et al. [^{11}C]PIB in a nondemented population: potential antecedent marker of Alzheimer disease. Neurology 2006;67:446–52.
[17] Fripp J, Bourgeat P, Acosta O, Raniga P, Modat M, Pike KE, et al. Appearance modeling of ^{11}C PiB PET images: characterizing amyloid deposition in Alzheimer's disease, mild cognitive impairment and healthy aging. Neuroimage 2008;43:430–9.
[18] Forsberg A, Engler H, Almkvist O, Blomquist G, Hagman G, Wall A, et al. PET imaging of amyloid deposition in patients with mild cognitive impairment. Neurobiol Aging 2008;29:1456–65.
[19] Okamura N, Suemoto T, Shimadzu H, Suzuki M, Shiomitsu T, Akatsu H, et al. Styrylbenzoxazole derivatives for in vivo imaging of amyloid plaques in the brain. J Neurosci, 2004;24:2535–41.
[20] Okamura N, Furumoto S, Funaki Y, Suemoto T, Kato M, Ishikawa Y, et al. Binding and safety profile of novel benzoxazole derivative for in vivo imaging of amyloid deposits in Alzheimer's disease. Geriatr Gerontol Int 2007;7:393–400.
[21] Furumoto S, Okamura N, Iwata R, Yanai K, Arai H, Kudo Y. Recent advances in the development of amyloid imaging agents. Curr Top Med Chem 2007;7:1773–89.
[22] Kudo Y, Okamura N, Furumoto S, Tashiro M, Furukawa K, Maruyama M, et al. 2-(2-[2-Dimethylaminothiazol-5-yl]Ethenyl)-6-(2-[Fluoro]Ethoxy)Benzoxazole: A novel PET agent for in vivo detection of dense amyloid plaques in Alzheimer's disease patients. J Nucl Med 2007;48:553–61.
[23] Fodero-Tavoletti MT, Mulligan RS, Okamura N, Furumoto S, Rowe CC, Kudo Y, et al. In vitro characterization of BF227 binding to α-synuclein/Lewy Bodies. Eur J Pharmacol 2009;617:54–8.
[24] Ishii K, Hashimoto M, Kimura Y, Sakata M, Oda K, Kawasaki K, et al. Direct comparison of in vivo accumulation of ^{11}C-PIB and ^{11}C-BF227 in Alzheimer's disease. Alzheimer's and Dementia, vol. 4, Issue 4; July 2008. p. T49. Supplement 1.
[25] Tiraboschi P, Hansen LA, Thal LJ, Corey-Bloom J. The importance of neuritic plaques and tangles to the development and evolution of AD. Neurology 2004;62:1984–9.
[26] Price JL, Morris JC. Tangles and plaques in nondemented aging and "preclinical" Alzheimer's disease. Ann Neurol 1999;45:358–68.
[27] Morris JC, Storandt M, Miller JP, McKeel DW, Price JL, Rubin EH, et al. Mild cognitive impairment represents early-stage Alzheimer disease. Arch Neurol 2001;58:397–405.
[28] Wang J, Dickson DW, Trojanowski JQ, Lee VM. The levels of soluble versus insoluble brain Abeta distinguish Alzheimer's disease from normal and pathologic aging. Exp Neurol 1999;158:328–37.
[29] Fox NC, Crum WR, Scahill RI, Stevens JM, Janssen JC, Rossor MN. Imaging of onset and progression of Alzheimer's disease with voxel-compression mapping of serial magnetic resonance images. Lancet 2001;358:201–5.
[30] Jack Jr CR, Shiung MM, Gunter JL, O'Brien PC, Weigand SD, Knopman DS, et al. Comparison of different MRI brain atrophy rate measures with clinical disease progression in AD. Neurology 2004;62:591–600.
[31] Karas GB, Scheltens P, Rombouts SA, Visser PJ, van Schijndel RA, Fox NC, et al. Global and local gray matter loss in mild cognitive impairment and Alzheimer's disease. Neuroimage 2004;23:708–16.
[32] Killiany RJ, Gomez-Isla T, Moss M, Kikinis R, Sandor T, Jolesz F, et al. Use of structural magnetic resonance imaging to predict who will get Alzheimer's disease. Ann Neurol 2000;47:430–9.
[33] Bell-McGinty S, Lopez OL, Meltzer CC, Scanlon JM, Whyte EM, Dekosky ST, et al. Differential cortical atrophy in subgroups of mild cognitive impairment. Arch Neurol 2005;62:1393–7.
[34] Chetelat G, Landeau B, Eustache F, Mezenge F, Viader F, de la Sayette V, et al. Using voxel-based morphometry to map the structural changes associated with rapid conversion in MCI: a longitudinal MRI study. Neuroimage 2005;27:934–46.
[35] Bozzali M, Filippi M, Magnani G, Cercignani M, Franceschi M, Schiatti E, et al. The contribution of voxel-based morphometry in staging patients with mild cognitive impairment. Neurology 2006;67:453–60.

[36] Hämäläinen A, Tervo S, Grau-Olivares M, Niskanen E, Pennanen C, Huuskonen J, et al. Voxel-based morphometry to detect brain atrophy in progressive mild cognitive impairment. Neuroimage 2007;37:1122–31.
[37] Karas G, Sluimer J, Goekoop R, van der Flier W, Rombouts SA, Vrenken H, et al. Amnestic mild cognitive impairment: structural MR imaging findings predictive of conversion to Alzheimer disease. Am J Neuroradiol 2008;29:944–9.
[38] Jack Jr CR, Lowe VJ, Senjem ML, Weigand SD, Kemp BJ, Shiung MM, et al. ^{11}C PiB and structural MRI provide complementary information in imaging of Alzheimer's disease and amnestic mild cognitive impairment. Brain 2008;131:665–80.
[39] McKhann G, Drachman D, Folstein M, Katzman R, Price D, Stadlan EM. Clinical diagnosis of Alzheimer's disease: report of the NINCDS-ADRDA Work Group under the auspices of Department of Health and Human Services Task Force on Alzheimer's Disease. Neurology 1984;34:939–44.
[40] Petersen RC, Smith GE, Waring SC, Ivnik RJ, Tangalos EG, Kokmen E. Mild cognitive impairment: clinical characterization and outcome. Arch Neurol 1999;56:303–8.
[41] Ashburner J, Friston KJ. Voxel-based morphometry—the methods. Neuroimage 2000;11:805–21.
[42] Hirata Y, Matsuda H, Nemoto K, Ohnishi T, Hirao K, Yamashita F, et al. Voxel-based morphometry to discriminate early Alzheimer's disease from controls. Neurosci Lett 2005;382:269–74.
[43] Pike KE, Savage G, Villemagne VL, Ng S, Moss SA, Maruff P, et al. Beta-amyloid imaging and memory in non-demented individuals: evidence for preclinical Alzheimer's disease. Brain 2007;130:2837–44.
[44] Engler H, Forsberg A, Almkvist O, Blomquist G, Larsson E, Savitcheva I, et al. Two-year follow-up of amyloid deposition in patients with Alzheimer's disease. Brain 2006;129:2856–66.
[45] Archer HA, Edison P, Brooks DJ, Barnes J, Frost C, Yeatman T, et al. Amyloid load and cerebral atrophy in Alzheimer's disease: an ^{11}C-PIB positron emission tomography study. Ann Neurol 2006;60:145–7.
[46] Josephs KA, Whitwell JL, Ahmed Z, Shiung MM, Weigand SD, Knopman DS, et al. Beta-amyloid burden is not associated with rates of brain atrophy. Ann Neurol 2008;63:204–12.

European Journal of Pharmacology 617 (2009) 54–58

Contents lists available at ScienceDirect

European Journal of Pharmacology

journal homepage: www.elsevier.com/locate/ejphar

Neuropharmacology and Analgesia

In vitro characterisation of BF227 binding to α-synuclein/Lewy bodies

Michelle T. Fodero-Tavoletti [a,b,c], Rachel S. Mulligan [f], Nobuyuki Okamura [e], Shozo Furumoto [d], Christopher C. Rowe [f], Yukitsuka Kudo [d], Colin L. Masters [c], Roberto Cappai [a,b,c], Kazuhiko Yanai [e], Victor L. Villemagne [a,c,f,*]

[a] Department of Pathology, The University of Melbourne, VIC, Australia
[b] Bio21 Molecular and Biotechnology Institute, The University of Melbourne, VIC, Australia
[c] The Mental Health Research Institute of Victoria, Tohoku University, Sendai, Japan
[d] Biomedical Engineering Research Organization, Tohoku University, Sendai, Japan
[e] Department of Pharmacology, Tohoku University, Sendai, Japan
[f] Department of Nuclear Medicine, Austin Health, Centre for PET, VIC, Australia

ARTICLE INFO

Article history:
Received 4 March 2009
Received in revised form 6 June 2009
Accepted 22 June 2009
Available online 1 July 2009

Keywords:
BF227
α-synuclein
Positron emission tomography
Dementia with Lewy bodies
Aβ (amyloid-β)
Imaging

ABSTRACT

Amyloid-β (Aβ) plaques are a pathological hallmark of Alzheimer's disease and a current target for positron emission tomography (PET) imaging agents. Whilst [^{11}C]-PiB is currently the most widely used PET ligand in clinic, a novel family of benzoxazole compounds have shown promise as Aβ imaging agents; particularly BF227. We characterised the in vitro binding of [^{18}F]-BF227 toward α-synuclein to address its selectivity for Aβ pathology, to establish whether [^{18}F]-BF227 binds to α-synuclein/Lewy bodies, in addition to Aβ plaques. In vitro [^{18}F]-BF227 saturation studies were conducted with 200 nM α-synuclein or $A\beta_{1-42}$ fibrils or 100 μg of Alzheimer's disease, pure dementia with Lewy bodies or control brain homogenates. Non-specific binding was established with PiB (1 μM). In vitro binding studies indicated that [^{18}F]-BF227 binds with high affinity to two binding sites on $A\beta_{1-42}$ fibrils (K_{D1} = 1.31 and K_{D2} = 80 nM, respectively) and to one class of binding sites on α-synuclein fibrils (K_D = 9.63nM). [^{18}F]-BF227 bound to Aβ-containing Alzheimer's disease brain (K_D = 25 ± 0.5 nM), but failed to bind to Aβ-free dementia with Lewy bodies or age-matched control homogenates. Moreover, BF227 labelled both Aβ plaques and Lewy bodies in immunohistochemical/fluorescence analysis of human Alzheimer's disease and Parkinson's disease brain sections, respectively. This study suggests that [^{18}F]-BF227 is not Aβ-selective. Evaluation of BF227 as a potential biomarker for Parkinson's disease is warranted.

1. Introduction

Currently, there is no cure for Alzheimer's disease, an age-related neurodegenerative disease, clinically characterised by dementia. The Alzheimer's disease brain is pathologically characterised by the presence of (i) extracellular amyloid plaques comprising amyloid-β (Aβ); (ii) intracellular neurofibrillary tangles composed of hyperphosphorylated tau; (iii) synaptic loss and reactive gliosis; (iv) increased oxidative damage to lipids, proteins and nucleic acids and (v) biometal dyshomeostasis (Goedert and Spillantini, 2006).

Definitive diagnosis of Alzheimer's disease and related dementias still relies upon postmortem examination. As new therapeutic strategies undergo clinical evaluation, considerable effort is now focused on biomarkers for the early and accurate diagnosis of Alzheimer's disease, as well as therapeutic monitoring. Modern molecular imaging procedures such as positron emission tomography (PET), may provide new insight into Alzheimer's disease by non-invasively identifying the underlying pathology of these diseases in the living. Of late, Pittsburgh compound B [PiB] has proven to be a successful biomarker for the in vivo quantitation of Aβ burden (Klunk et al., 2004; Rowe et al., 2007). Nonetheless, its widespread clinical use is impracticable due to the 20-minute decay half-life of carbon-11, limiting its use to centres with an on-site cyclotron. [^{18}F]-FDDNP also highlights Aβ deposits in the human brain; however, FDDNP also binds to neurofibrillary tangles (Agdeppa et al., 2001), as well as PrP^{sc} (Boxer et al., 2007; Bresjanac et al., 2003). Whilst labelling with a longer half-life isotope [^{18}F] proves to be advantageous, FDDNP's lack of selectivity considerably reduces its ability to provide differential diagnosis of neurodegenerative diseases. Hence, the development of a specific

* Corresponding author. Department of Nuclear Medicine, Austin Health, Centre for PET 145 Studley Rd Heidelberg, VIC, 3084 Australia. Tel.: +61 3 9496 3321; fax: +61 3 9458 5023.
E-mail address: villemagne@petnm.unimelb.edu.au (V.L. Villemagne).

0014-2999/$ – see front matter © 2009 Elsevier B.V. All rights reserved.
doi:10.1016/j.ejphar.2009.06.042

and selective [^{18}F]-labelled imaging agent(s) for molecular Aβ imaging is highly desirable to improve diagnostic accuracy and accelerate discovery and monitoring of therapeutics.

Recently, a novel series of benzoxazole compounds have been developed as PET imaging agents; namely BF227 [2-[2-(2-dimethylaminothiazol-5-yl)ethenyl]-6-[2-(fluoro)ethoxy] benzoxazole] has been demonstrated to bind to $A\beta_{1-42}$ fibrils (with low nanomolar affinity) and Aβ plaques in Alzheimer's disease brain sections (Kudo et al., 2007). [^{11}C]-BF227-PET demonstrated retention in cerebral cortices of Alzheimer's disease patients with very little retention in normal patients; suggesting BF227 as a promising PET imaging agent for the in vivo detection of Aβ pathology in Alzheimer's disease patients. Whilst the specificity of BF227 binding to Aβ has been established, there is limited knowledge regarding its selectivity; particularly since Alzheimer's disease has been described as a 'triple brain amyloidosis' (Trojanowski, 2002), comprising Aβ, tau and α-synuclein that when misfolded, comprise the principal components of senile plaques, neurofibrillary tangles and Lewy bodies. Furthermore, the majority of dementia with Lewy bodies cases exhibit extensive cortical Aβ deposition along the pathognomonic Lewy bodies (McKeith et al., 2005). Hence, critical assessment of new radiotracers such as BF227 is warranted to avoid misinterpretation of results and/or incorrect diagnosis. Whilst BF227 binding to neurofibrillary tangles has previously been examined (Kudo et al., 2007), the potential of BF227 binding to α-synuclein has not been assessed. The aim of this study was to test the ability of BF227 to bind/recognise α-synuclein fibrils/Lewy bodies to establish whether [^{18}F]-BF227 is selective for Aβ pathology.

2. Materials and methods

2.1. Materials

All reagents were purchased from Sigma (St. Louis, MO), unless otherwise stated. Human $A\beta_{1-42}$ was purchased from the W. M. Keck Laboratory (Yale University, New Haven, CT).

2.1.1. Tissue collection and characterisation

Brain tissue was collected at autopsy. The sourcing and preparation of the human brain tissue were conducted by the National Neural Tissue Resource Centre. Alzheimer's disease pathological diagnosis was made according to standard NIA-Reagan Institute criteria (1997). Dementia with Lewy bodies cases was diagnosed using consensus guidelines (McKeith et al., 1996) and classified as either dementia with Lewy bodies-Aβ, being subjects with evidence of neuritic plaques and/or cerebral vascular amyloid, as determined by IHC and ELISA, or pure dementia with Lewy bodies (no significant evidence of neuritic plaques and/or cerebral vascular amyloid). Parkinson's disease pathological diagnosis was made following previously described criteria (Braak et al., 2003; Forno, 1996). Determination of age-matched controls cases were also subject to the above criteria. The number of subject cases utilised is indicated in the figure/table texts. Overall, three Alzheimer's disease, three dementia with Lewy bodies-Aβ, one pure Dementia with Lewy bodies, two Parkinson's disease and three age-matched control subjects were utilised in this study.

2.1.2. [^{18}F] labelling of BF227

Unlabelled BF227 and 2-[2-(2-dimethylaminothiazol-5-yl)ethenyl]-6-[2-(tosyloxy)ethoxy] benzoxazole (BF-226; the precursor for [^{18}F]-BF-227) were custom synthesised by Tanabe R&D Service Co. and confirmed for purity by reverse phase high performance liquid chromatography, one dimensional NMR and mass spectrometry. [^{18}F]-BF227 was synthesised by nucleophilic substitution of the tosylate precursor (BF-226) (see below). Following a 10 min reaction at 110°C the crude reaction was partially purified on an activated Sep Pak tC18 cartridge before undergoing semi preparative reverse phase HPLC purification. Standard tC18 Sep-Pak reformulation produced [^{18}F]-BF227 in >95% radiochemical purity. The radiochemical yield was 17% (non decay corrected) and at the end of the synthesis the average specific activity was 1471 mCi/μmol/42 GBq/μmol.

Schematic for the radiosynthesis of [^{18}F]-BF227.

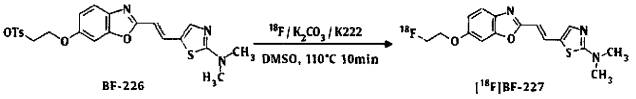

2.1.3. Preparation of amyloid fibrils

Synthetic $A\beta_{1-42}$ was dissolved in 1× PBS pH 7.7 to a final concentration of 200 μM. Recombinant human α-synuclein was expressed and purified as previously described (Cappai et al., 2005) and dissolved in 10 mM phosphate buffer pH 7.4, to a final concentration of 200 μM. These solutions were incubated at 37°C for either 2 days for $A\beta_{1-42}$ or 7 days for α-synuclein, with agitation (220 rpm, Orbital mixer incubator, Ratek). After aggregation, approximately 5% of the protein remained in the supernatant after centrifugation at 12,000×g for 20 minutes. Fibril aggregation was confirmed through ThT fluorescence spectroscopy and electron microscopy.

2.1.4. Preparation of human brain tissue for in vitro binding studies

Grey matter was isolated from the postmortem frontal cortex tissue from the Alzheimer's disease, dementia with Lewy bodies-Aβ, pure dementia with Lewy bodies and age-matched control subjects. Isolated tissue was then homogenised in 1× PBS (without calcium and magnesium), utilising an ultrasonic cell disrupter (2 × 30 s, 24,000 rpm; Virsonic 600, Virtis). Protein concentration was determined using the BCA protein assay (Pierce) and brain tissue homogenates were aliquoted and frozen at −80 °C until used.

2.1.5. In vitro BF227 binding assays

Synthetic $A\beta_{1-42}$ or α-synuclein fibrils (200 nM) were incubated with increasing concentrations of [^{18}F]-BF227 (0.5–200 nM). To account for non-specific binding of [^{18}F]-BF227, the above mentioned reactions were duplicated in the presence of unlabelled 1 μM PiB. The binding reactions were incubated for 1 h at room temperature in 200 μl of assay buffer [PBS, minus Mg^{2+} and Ca^{2+} (JRH Biosciences, Kansas, USA); 0.1% BSA]. Binding of [^{18}F]-BF227 to human brain homogenates was assessed by incubating 100 μg brain homogenate from Alzheimer's disease, pure dementia with Lewy bodies (Aβ-free) and age-matched control subjects with increasing concentrations of [^{18}F]-BF227 (0.1–250nM [^{18}F]-BF227 in the absence or presence of unlabelled PiB (1 μM)), as described above. Bound from free radioactivity was separated by filtration under reduced pressure (MultiScreen HTS Vacuum Manifold; MultiScreen HTS 96-well filtration plates; 0.65 μm, Millipore). Filters were washed three times with 200 μl assay buffer and incubated overnight in 3 ml scintillation fluid. Washed filters were assayed for radioactivity in an automatic gamma counter (Wallac 1480 Wizard 3″; Perkin Elmer). Binding data were analysed with curve fitting software that calculates the K_D and B_{max} using nonlinear regression according to the equation:

$$Y = B_{max} \cdot X$$

$$K_D + X$$

(GraphPad Prism Version 1.0, GraphPad Software, San Diego, CA). All experiments were conducted in triplicate.

2.2. Immunohistochemistry (IHC) and Fluorescence Analysis

Brain tissue from Alzheimer's disease and Parkinson's disease subjects was fixed in 10% formalin/PBS and embedded in paraffin. For immunohistochemistry and fluorescence analysis of BF227, 7 μm serial sections were assessed. Serial sections were deparaffinized and treated with 80% formic acid for 5 min and endogenous peroxidase

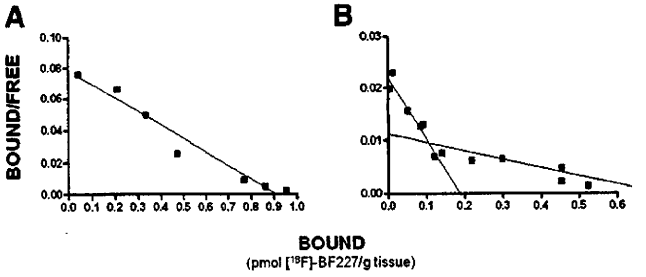

Fig. 1. In vitro binding studies indicate one class of [^{18}F]-BF227 binding sites on α-synuclein fibrils. Scatchard plots of [^{18}F]-BF227 binding to synthetic (A) α-synuclein or (B) $A\beta_{1-42}$ fibrils. (A) Scatchard analysis identified one class of BF227 binding sites on α-synuclein fibrils (K_D of 9.63 nM and B_{max} of 2.76 pmol BF227/nmol α-synuclein). (B) Scatchard analysis identified two classes of BF227 binding sites on $A\beta_{1-42}$; a high affinity binding site with K_D and B_{max} of 1.31 nM and 0.171 pmol BF227/nmol $A\beta_{1-42}$, respectively and a low affinity binding site with K_D and B_{max} of 80.0 nM and 2.96 pmol BF227/nmol $A\beta_{1-42}$, respectively. Binding data were analysed using GraphPad Software (Version 1.0, San Diego, CA). This figure is the average of at least three independent experiments.

activity was blocked utilising 3% hydrogen peroxide. Serial tissue sections were stained in the following order: the first and third sections were immunostained with 97/8 or 1e8 antibodies to identify Lewy bodies or Aβ plaques, respectively and the second section was incubated with BF227. For immunostaining, sections were treated with blocking buffer (20% fetal calf serum, 50 mM Tris–HCl, 175 mM NaCl pH 7.4) before immunostaining with primary antibodies to α-synuclein [97/8; 1:2000 dilution (Culvenor et al., 1999)] or Aβ (1e8; 1:50), for 1 h at room temperature. Visualisation of antibody reactivity was achieved using the LSAB™ kit (labelled streptavidin–biotin, DAKO) and sections were then incubated with hydrogen-peroxidase–diaminobenzidine (H_2O_2–DAB) to visualise the α-synuclein or Aβ-positive deposits. Sections were counterstained with Mayer's hematoxylin. To assess BF227 fluorescence, quenching to minimise autofluorescence was first performed on deparaffinized tissue sections by treatment with 0.25% $KMnO_4$/PBS for 20 min prior to washing (PBS) and incubation with 1% potassium metabisulfite/1% oxalic acid/PBS for 5 min. Following autofluorescence quenching, sections were blocked in 2% BSA/PBS pH 7.0 for 10 min and stained with 100 μM BF227 for 30 min. Washed (PBS) sections were then mounted in non-fluorescent mounting media (DAKO). Epifluorescence images were visualised using a Zeiss microscope (47CFP; filter set 47 (EM BP 436/20, BS FT 455, EM BP480/40). Co-localisation of the BF227 and antibody signals was assessed by overlaying images from each of the stained serial tissue sections.

3. Results

3.1. Characteristics of [^{18}F]-BF227 Binding to Recombinant α-Synuclein and $A\beta_{1-42}$ Fibrils

To investigate the selectivity of BF227, we tested the ability of [^{18}F]-BF227 to bind to synthetic α-synuclein and $A\beta_{1-42}$ fibrils; the major component of Lewy bodies and senile plaques, respectively. The successful formation of fibrils was determined by ThT fluorescence and transmission electron microscopy, prior to conducting the binding assays (data not shown).

Assessment of [^{18}F]-BF227 binding was conducted using equimolar concentrations (200 nM, ~4.0×10^{-11} mol) of either α-synuclein or $A\beta_{1-42}$ fibrils. Scatchard analysis indicated that [^{18}F]-BF227 bound to one site on α-synuclein fibrils with high affinity (K_D 9.63nM; Fig. 1A). In contrast, two classes of binding sites exist for [^{18}F]-BF227 binding to $A\beta_{1-42}$ fibrils (high affinity K_{D1} 1.31 and low affinity K_{D2} 80nM, respectively; Fig. 1B). Despite the two classes of binding sites identified for $A\beta_{1-42}$ fibrils, the total number of binding sites was similar for both α-synuclein (B_{max} 2.76 pmol [^{18}F]-BF227/nmol α-synuclein) and $A\beta_{1-42}$ (B_{max1} 0.171 and B_{max2} 2.96 pmol [^{18}F]-BF227/nmol $A\beta_{1-42}$) fibrils.

3.2. In Vitro [^{18}F]-BF227 Binding Analysis of Human Alzheimer's Disease and Dementia With Lewy Bodies Brain

In previous studies, postmortem human brain homogenates have been extensively utilised to characterise amyloid imaging agents, including PiB (Fodero-Tavoletti et al., 2007; Klunk et al., 1995; Klunk et al., 2003; Klunk et al., 2005; Mathis et al., 2003). To further assess the selectivity of BF227, we compared the in vitro binding properties of [^{18}F]-BF227 to Aβ-containing brain homogenates (Alzheimer's disease) versus Aβ-free (non-detectable levels of Aβ) homogenates (pure dementia with Lewy bodies and age-matched control). Aβ ELISA analysis was utilised to establish the presence/absence (non-detectable levels) of Aβ, prior to conducting binding studies (data not shown). [^{18}F]-BF227 bound with high affinity to Aβ-containing brain homogenates. Scatchard analysis identified one class of binding sites within Alzheimer's disease homogenates with a K_D of 33 ± 4.8 nM and a B_{max} of 9353 pmol/[^{18}F]-BF227/g tissue (Fig. 2A). In contrast, [^{18}F]-BF227 did not bind to the α-synuclein-containing Aβ-free dementia with Lewy bodies (dementia with Lewy bodies-pure; Fig. 2B) or the Aβ-and α-synuclein-free age-matched control subjects (Fig. 2C).

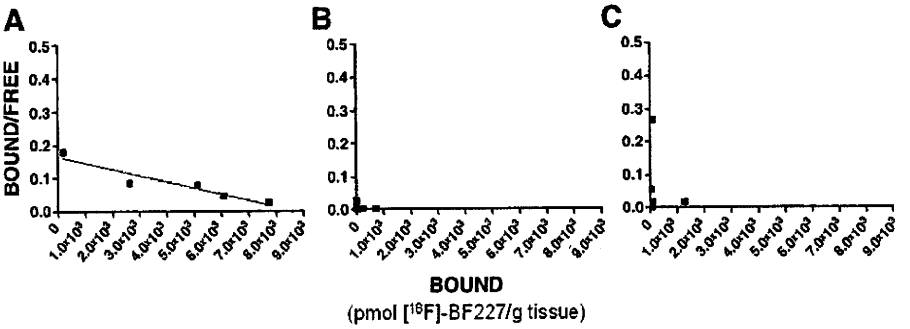

Fig. 2. In vitro binding studies demonstrate that [^{18}F]-BF227 fails to bind to pure dementia with Lewy bodies brain homogenate. Scatchard plots of [^{18}F]-BF227 binding to (A) AD, (B) age-matched control and (C) pure dementia with Lewy bodies brain homogenates. Scatchard analysis indicated that BF227 binds to Alzheimer's disease (K_D 33 ± 4.8nM, B_{max} 9353 pmol/[^{18}F]-BF227/g tissue). No significant binding of [^{18}F]-BF227/g to pure dementia with Lewy body or age-matched control subjects was observed. Binding data were analysed using GraphPad Software (Version 1.0, San Diego, CA). This figure is the average of at least three independent experiments.

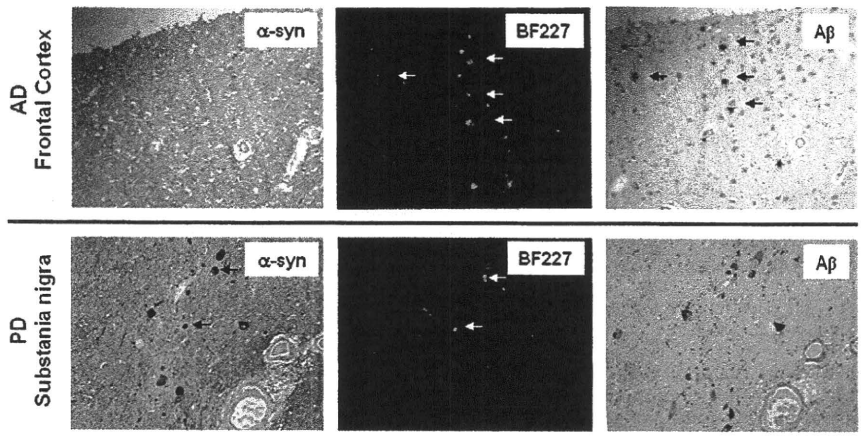

Fig. 3. Immunohistochemistry analysis indicates that BF227 binds specifically to Aβ plaques and not α-synuclein-containing Lewy bodies within the substantia nigra. Microscopy images of three serial sections (7 mm) from the frontal cortex of (A) Alzheimer's disease or (B) substantia nigra Parkinson's disease brain, immunostained with antibodies to α-synuclein (97/8; 1:2000) and Aβ (1E8; 1:50), to identify Lewy bodies and Aβ plaques respectively; or stained with 100 mM BF227. Black arrows indicate the location of Aβ plaques (top panel) and Lewy bodies (bottom panel), as determined by immunohistochemistry. White arrows indicate positive BF227 staining as detected by fluorescence, co-localising with 1E8 immunostaining of Aβ plaques in Alzheimer's disease subjects and Lewy bodies in the substantia nigra of Parkinson's disease subjects. Tissue sections were imaged using a Leica microscope and Axiocam digital camera. Scale bars, 50 mm.

3.3. BF227 and Immunohistochemical Staining of Human Alzheimer's Disease and Parkinson's Disease Subjects

As a qualitative measure of its potential binding to α-synuclein deposits/Lewy bodies by fluorescence microscopy, unlabelled BF227 was used to stain fixed serial sections from the substantia nigra of Parkinson's disease subjects. Staining of the frontal cortex of Alzheimer's disease subjects was also conducted. Parkinson's disease substantia nigra sections were chosen for their rich source of Lewy bodies. BF227 staining of the substantia nigra co-localised with immuno-reactive α-synuclein-containing Lewy bodies (Fig. 3). A comparison of the α-synuclein staining Lewy bodies with BF227 staining suggested that BF227 binds to Lewy bodies as well as Aβ stained plaques.

4. Discussion

The ongoing quest for specific and selective PET imaging agents is imperative for the early diagnosis, treatment, development and monitoring of neurodegenerative diseases, such as Alzheimer's disease. To date, the design and testing of PET imaging candidates have suggested that compounds based on histological dyes whilst specific, are not selective for Aβ pathology. Benzoxazole compounds/derivatives represent a promising new family of imaging agents that may overcome some of the limitations of current PET ligands.

In vitro binding studies indicated that [^{18}F]-BF227 bound significantly to $A\beta_{1-42}$ fibrils; exhibiting two classes of binding sites. Previous studies (Kudo et al., 2007) assessing the binding affinity of BF227 to $A\beta_{1-42}$ fibrils utilised a competition binding assay that was incapable of detecting multiple classes of binding sites. This study is the first to suggest the existence of two binding sites for benzoxazole compounds on $A\beta_{1-42}$ fibrils. Binding of [^{18}F]-BF227 to α-synuclein fibrils was observed only at an equimolar concentration to $A\beta_{1-42}$ fibrils although, with a ~10-fold lower affinity when compared to $A\beta_{1-42}$ fibrils (Fig. 1A). The lower affinity of [^{18}F]-BF227 for synthetic α-synuclein fibrils as compared to $A\beta_{1-42}$ fibrils and the concentration of [^{18}F]-BF227 (~1 nM) typically achieved during PET studies, suggests that the binding of [^{18}F]-BF227 to α-synuclein-containing Lewy bodies should not contribute significantly to the [^{18}F]-BF227-PET signal.

Despite the results obtained for synthetic $A\beta_{1-42}$ fibrils, in vitro studies in brain homogenates failed to show two binding sites. Nevertheless, a high affinity K_D value in the low nanomolar range was observed. This distinction may reflect the fact that Aβ plaques are not only composed of $A\beta_{1-42}$, but also $A\beta_{1-40}$ and other longer or truncated species of Aβ (i.e. $A\beta_{1-39}$ and $A\beta_{1-43}$) within the Alzheimer's disease brain. Despite the binding of [^{18}F]-BF227 to α-synuclein fibrils, no binding of [^{18}F]-BF227 was detected in pure dementia with Lewy bodies homogenates, devoid of Aβ plaques. This observation may indicate that the density of α-synuclein-containing Lewy bodies present in the pure dementia with Lewy bodies homogenates analysed may be low and therefore undetectable by [^{18}F]-BF227. Our previous studies assessing PiB binding to α-synuclein fibrils and pure dementia with Lewy bodies brain homogenates yielded similar results and as remarked there, the concentration of α-synuclein fibrils utilised for the in vitro studies may be physiologically unattainable, explaining the discrepancy between fibril and dementia with Lewy bodies brain homogenate results (Fodero-Tavoletti et al., 2007).

Consistent with previous reports, BF227 staining of Aβ plaques was clearly evident in the Alzheimer's disease brain sections examined. Fluorescence studies also demonstrated that BF227 bound to Lewy bodies, as indicated by the co-localisation of BF227 staining with α-synuclein-positive Lewy bodies (Fig. 3). Noteworthy, the concentration of BF227 used for the fluorescent studies was considerably higher (100 μM) that the low nanomolar concentrations typically achieved during in vivo PET studies (Kudo et al., 2007).

In conclusion this study supports the notion that [^{18}F]-BF227 is not entirely selective for Aβ pathology. Whilst previous PET studies were conducted using the carbon-11 labelled BF227, we anticipate that our results would be applicable to both [^{11}C]- and [^{18}F]-labelled BF227 PET studies, as the chemical nature of BF227 is not altered using either radioisotope. Therefore, taking into consideration the calculated K_D for α-synuclein fibrils and the size and cortical density of Lewy bodies, we speculate that the potential contribution of Lewy bodies to [^{11}C]-BF227-PET retention in the brains of Alzheimer's disease and even dementia with Lewy bodies patients (when assessed), should be considered to be extremely low. Nevertheless, given the high affinity for α-synuclein, added to the high density of Lewy bodies in the substantia nigra of most Parkinson's disease patients, evaluation of BF227 as a Parkinson's disease diagnostic biomarker, does warrant further investigation.

Acknowledgments

The authors would like to thank Prof. Catriona McLean, Fairlie Hinton and Geoff Pavey from the National Neural Tissue Resource

Centre for sourcing and preparation of the human brain tissue. We acknowledge the funding from the National Health and Medical Research Council and Ministry of Health, Labour and Welfare, Japan. RC is an NHMRC Senior Research Fellow.

References

Agdeppa, E.D., Kepe, V., Liu, J., Flores-Torres, S., Satyamurthy, N., Petric, A., Cole, G.M., Small, G.W., Huang, S.C., Barrio, J.R., 2001. Binding characteristics of radiofluorinated 6-dialkylamino-2-naphthylethylidene derivatives as positron emission tomography imaging probes for beta-amyloid plaques in Alzheimer's disease. J. Neurosci. 21, RC189.

Boxer, A.L., Rabinovici, G.D., Kepe, V., Goldman, J., Furst, A.J., Huang, S.C., Baker, S.L., O'Neil, J.P., Chui, H., Geschwind, M.D., Small, G.W., Barrio, J.R., Jagust, W., Miller, B.L., 2007. Amyloid imaging in distinguishing atypical prion disease from Alzheimer disease. Neurology 69, 283–290.

Braak, H., Del Tredici, K., Rub, U., de Vos, R.A., Jansen Steur, E.N., Braak, E., 2003. Staging of brain pathology related to sporadic Parkinson's disease. Neurobiol Aging 24, 197–211.

Bresjanac, M., Smid, L.M., Vovko, T.D., Petric, A., Barrio, J.R., Popovic, M., 2003. Molecular-imaging probe 2-(1-[6-[(2-fluoroethyl)(methyl) amino]-2-naphthyl]ethylidene) malononitrile labels prion plaques in vitro. J Neurosci 23, 8029–8033.

Cappai, R., Leck, S.L., Tew, D.J., Williamson, N.A., Smith, D.P., Galatis, D., Sharples, R.A., Curtain, C.C., Ali, F.E., Cherny, R.A., Culvenor, J.G., Bottomley, S.P., Masters, C.L., Barnham, K.J., Hill, A.F., 2005. Dopamine promotes alpha-synuclein aggregation into SDS-resistant soluble oligomers via a distinct folding pathway. FASEB. J. 19, 1377–1379.

Culvenor, J.G., McLean, C.A., Cutt, S., Campbell, B.C., Maher, F., Jakala, P., Hartmann, T., Beyreuther, K., Masters, C.L., Li, Q.X., 1999. Non-Abeta component of Alzheimer's disease amyloid (NAC) revisited. NAC and alpha-synuclein are not associated with Abeta amyloid. Am. J. Pathol. 155, 1173–1181.

Fodero-Tavoletti, M.T., Smith, D.P., McLean, C.A., Adlard, P.A., Barnham, K.J., Foster, L.E., Leone, L., Perez, K., Cortes, M., Culvenor, J.G., Li, Q.X., Laughton, K.M., Rowe, C.C., Masters, C.L., Cappai, R., Villemagne, V.L., 2007. In vitro characterization of Pittsburgh compound-B binding to Lewy bodies. J. Neurosci. 27, 10365–10371.

Forno, L.S., 1996. Neuropathology of Parkinson's disease. J. Neuropathol. Exp. neurol. 55, 259–272.

Goedert, M., Spillantini, M.G., 2006. A century of Alzheimer's disease. Science. (New. York,. N.Y. 314, 777–781.

Klunk, W.E., Debnath, M.L., Pettegrew, J.W., 1995. Chrysamine-G binding to Alzheimer and control brain: autopsy study of a new amyloid probe. Neurobiol. Aging. 16, 541–548.

Klunk, W.E., Engler, H., Nordberg, A., Bacskai, B.J., Wang, Y., Price, J.C., Bergstrom, M., Hyman, B.T., Langstrom, B., Mathis, C.A., 2003. Imaging the pathology of Alzheimer's disease: amyloid-imaging with positron emission tomography. Neuroimaging Clinics of North America 13, 781–789, ix.

Klunk, W.E., Engler, H., Nordberg, A., Wang, Y., Blomqvist, G., Holt, D.P., Bergstrom, M., Savitcheva, I., Huang, G.F., Estrada, S., Ausen, B., Debnath, M.L., Barletta, J., Price, J.C., Sandell, J., Lopresti, B.J., Wall, A., Koivisto, P., Antoni, G., Mathis, C.A., Langstrom, B., 2004. Imaging brain amyloid in Alzheimer's disease with Pittsburgh compound-B. Ann. Neurol. 55, 306–319.

Klunk, W.E., Lopresti, B.J., Ikonomovic, M.D., Lefterov, I.M., Koldamova, R.P., Abrahamson, E.E., Debnath, M.L., Holt, D.P., Huang, G.F., Shao, L., DeKosky, S.T., Price, J.C., Mathis, C.A., 2005. Binding of the positron emission tomography tracer Pittsburgh compound-B reflects the amount of amyloid-beta in Alzheimer's disease brain but not in transgenic mouse brain. J. Neurosci. 25, 10598–10606.

Kudo, Y., Okamura, N., Furumoto, S., Tashiro, M., Furukawa, K., Maruyama, M., Itoh, M., Iwata, R., Yanai, K., Arai, H., 2007. 2-(2-[2-Dimethylaminothiazol-5-yl]ethenyl)-6-(2-[fluoro]ethoxy)benzoxazole: a novel PET agent for in vivo detection of dense amyloid plaques in Alzheimer's disease patients. J. Nucl. Med. 48, 553–561.

Mathis, C.A., Wang, Y., Holt, D.P., Huang, G.F., Debnath, M.L., Klunk, W.E., 2003. Synthesis and evaluation of 11C-labeled 6-substituted 2-arylbenzothiazoles as amyloid imaging agents. J. Medicinal. Chem. 46, 2740–2754.

McKeith, I.G., Dickson, D.W., Lowe, J., Emre, M., O'Brien, J.T., Feldman, H., Cummings, J., Duda, J.E., Lippa, C., Perry, E.K., Aarsland, D., Arai, H., Ballard, C.G., Boeve, B., Burn, D.J., Costa, D., Del Ser, T., Dubois, B., Galasko, D., Gauthier, S., Goetz, C.G., Gomez-Tortosa, E., Halliday, G., Hansen, L.A., Hardy, J., Iwatsubo, T., Kalaria, R.N., Kaufer, D., Kenny, R.A., Korczyn, A., Kosaka, K., Lee, V.M., Lees, A., Litvan, I., Londos, E., Lopez, O.L., Minoshima, S., Mizuno, Y., Molina, J.A., Mukaetova-Ladinska, E.B., Pasquier, F., Perry, R.H., Schulz, J.B., Trojanowski, J.Q., Yamada, M., 2005. Diagnosis and management of dementia with Lewy bodies: third report of the DLB Consortium. Neurology 65, 1863–1872.

McKeith, I.G., Galasko, D., Kosaka, K., Perry, E.K., Dickson, D.W., Hansen, L.A., Salmon, D.P., Lowe, J., Mirra, S.S., Byrne, E.J., Lennox, G., Quinn, N.P., Edwardson, J.A., Ince, P.G., Bergeron, C., Burns, A., Miller, B.L., Lovestone, S., Collerton, D., Jansen, E.N., Ballard, C., de Vos, R.A., Wilcock, G.K., Jellinger, K.A., Perry, R.H., 1996. Consensus guidelines for the clinical and pathologic diagnosis of dementia with Lewy bodies (DLB): report of the Consortium on DLB International Workshop. Neurology 47, 1113–1124.

Rowe, C.C., Ng, S., Ackermann, U., Gong, S.J., Pike, K., Savage, G., Cowie, T.F., Dickinson, K.L., Maruff, P., Darby, D., Smith, C., Woodward, M., Merory, J., Tochon-Danguy, H., O'Keefe, G., Klunk, W.E., Mathis, C.A., Price, J.C., Masters, C.L., Villemagne, V.L., 2007. Imaging beta-amyloid burden in aging and dementia. Neurology 68, 1718–1725.

Trojanowski, J.Q., 2002. Emerging Alzheimer's disease therapies: focusing on the future. Neurobiol. Aging. 23, 985–990.

Imaging Amyloid Pathology in the Living Brain

Nobuyuki Okamura[a,*], Shozo Furumoto[b], Hiroyuki Arai[c], Ren Iwata[d], Kazuhiko Yanai[a] and Yukitsuka Kudo[b]

[a]*Department of Pharmacology, Tohoku University School of Medicine, Sendai 980-8575, Japan,* [b]*Tohoku University Biomedical Engineering Research Organization (TUBERO), Sendai 980-8575, Japan,* [c]*Center for Asian Traditional Medicine, Department of Geriatrics and Gerontology, Tohoku University School of Medicine, Sendai 980-8574, Japan,* [d]*Division of Radiopharmaceutical Chemistry, Cyclotron and Radioisotope Center, Tohoku University, Sendai 980-8578, Japan*

Abstract: Progressive deposition of amyloid plaques in the brain, which begins before the appearance of cognitive decline, is an initiating event in the pathogenesis of Alzheimer's disease. Therefore, noninvasive detection of amyloid pathology is important for presymptomatic diagnosis and preventive therapy for Alzheimer's disease. Recent research advances have enabled the *in vivo* imaging of amyloid pathology in humans using nuclear medicine technology. Several amyloid-binding agents have been developed and evaluated by positron emission tomography (PET) and single photon emission computed tomography (SPECT) for their use as contrast agents. Available clinical evidence indicates that amyloid imaging enables the early diagnosis of Alzheimer's disease with high accuracy and suggests its usefulness for the prediction of progression to Alzheimer's disease in subjects with mild cognitive impairment and probably also in cognitively normal individuals. Another application of this technology is as a surrogate marker for monitoring brain amyloid. In this review, we describe recent progress in the development of amyloid imaging technology and human clinical trials.

Keywords: Amyloid, Alzheimer's disease, Positron emission tomography (PET), molecular imaging, senile plaque, neurofibrillary tangle.

INTRODUCTION

Alzheimer's disease (AD) is the most common cause of dementia in the elderly. The definitive diagnosis of AD relies on postmortem assessment, with characteristic pathological changes such as neuron death, senile plaques (SPs), and neurofibrillary tangles (NFTs). Currently, the amyloid cascade hypothesis is widely accepted to account for the pathogenesis of AD [1]. SP is mainly composed of amyloid β (Aβ), which is generated by proteolytic reaction of β and γ-secretase from the amyloid precursor protein (APP). In this hypothesis, the mismetabolism of APP is the initiating event in AD pathogenesis. Excessive generation of Aβ causes aggregation of Aβ and the formation of SPs, and this is followed by the formation of NFTs, neuron death, neurotransmitter deficit, and cognitive decline. If this hypothesis is correct, optimal therapeutic strategies for interrupting the disease process should be directed toward modifying the generation, clearance, and cytotoxicity of Aβ.

Early diagnosis and treatment of AD is important in maintaining the patient's activities of daily living as long as possible and preventing the patient from becoming bedridden. A notable feature of AD is a discrepancy between clinical symptoms and pathological findings in the brain (Fig. (1)). Even in the clinically early stage of dementia, a large amount of SP is already present in the brain [2, 3]. These changes in the brain probably start 10–20 years before clinical symptoms appear. Therefore, if the deposition of SPs in the brain can be measured noninvasively, subjects who are certain to develop AD (i.e., "preclinical AD") could be screened as candidates for preventive therapy.

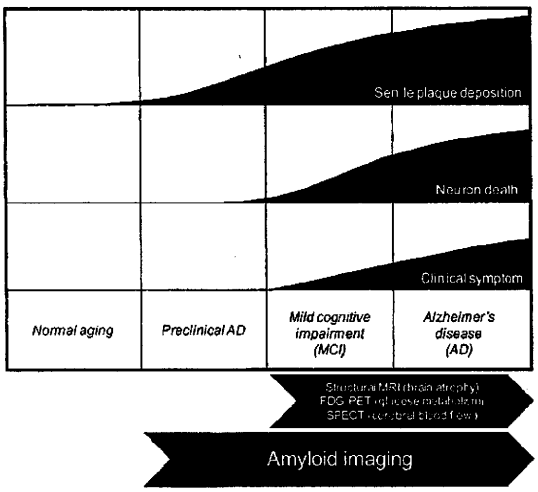

Fig. (1). Senile plaque deposition, neuron death and clinical symptom of Alzheimer's disease.

Recently, several imaging techniques, including positron emission tomography (PET), single photon emission computed tomography (SPECT), magnetic resonance imaging, and near-infrared imaging, have been developed for the noninvasive detection of SPs in AD patients. These techniques, recently classified as "amyloid imaging", are considered ideal for screening candidates for anti-amyloid therapy. PET is the most popular method for amyloid

*Address correspondence to this author at the Department of Pharmacology, Tohoku University School of Medicine, 2-1, Seiryo-machi, Aoba-ku, Sendai 980-8575, Japan; Tel: + 81-22-717-8058; Fax: +81-22-717-8060; E-mail: oka@mail.tains.tohoku.ac.jp

1573-4056/08 $55.00+.00

imaging, because of its advantages of high sensitivity, good spatial resolution, quantitative results, and ease of probe development.

DEVELOPMENT OF AMYLOID-IMAGING AGENTS

Recent advances in molecular imaging have enabled the noninvasive detection of amyloid deposits by PET or SPECT. For the high-contrast detection of amyloid deposits, imaging agents should have high binding affinity for Aβ fibrils and substantial permeability through the blood–brain barrier (BBB). Several amyloid-binding agents have been developed for the *in vivo* detection of amyloid deposits (Fig. (2)). The development of these agents started with the use of Congo red, which is commonly used for the histochemical staining of amyloid [4]. However, the BBB permeability of Congo red is limited because of its molecular size and electrostatic charge. Therefore, several Congo red derivatives have been developed with improved BBB permeability without reduced binding to amyloid [5-8]. Chrysamine-G is the first Congo red derivative that has been examined as an *in vivo* amyloid-imaging probe. However, entry of this compound into the brain is limited. Other derivatives, including BSB, ISB, and methoxy-X04, have also been developed to improve the BBB permeability. BSB successfully visualizes brain amyloid deposits in APP-transgenic mice after intravenous administration of the compound. However, this compound has insufficient BBB permeability for it to be useful as a clinical PET tracer. The first successful amyloid imaging agent to have been administered to humans is 2-(1-{6-[(2-[^{18}F]fluoroethyl)(methyl)amino]-2-naphthyl}ethylidene)malononitrile ([^{18}F]FDDNP) [9]. One of the characteristics of this agent is its ability to bind both SPs and NFTs in the AD brain. In addition, this compound is extremely lipophilic; therefore, it can penetrate the BBB more easily than previously reported compounds [10]. Interestingly, this compound binds to the same site in Aβ fibrils as non-steroidal anti-inflammatory drugs (NSAIDs) do. Therefore, this agent enables us to determine the occupancy rate of NSAIDs and experimental drugs in SPs [11]. Other candidate amyloid-imaging agents include thioflavin-T derivatives [12, 13]. N-methyl-[^{11}C]2-(4'-methylaminophenyl)-6-hydroxybenzothiazole ([^{11}C]PIB) is one such derivative and is currently the most successful amyloid-imaging agent. This compound shows high binding affinity for Aβ fibrils and SPs in AD brain homogenates, in contrast to low binding affinity for NFTs [14]. After intravenous administration, this agent shows high BBB permeability and rapid washout from normal brain tissue. Other amyloid-imaging agents, such as IMPY, stilbene, benzofuran, and acridine orange derivatives, have also been explored for use as PET and SPECT imaging probes [15-19]. The iodinated agent IMPY has been explored as a SPECT

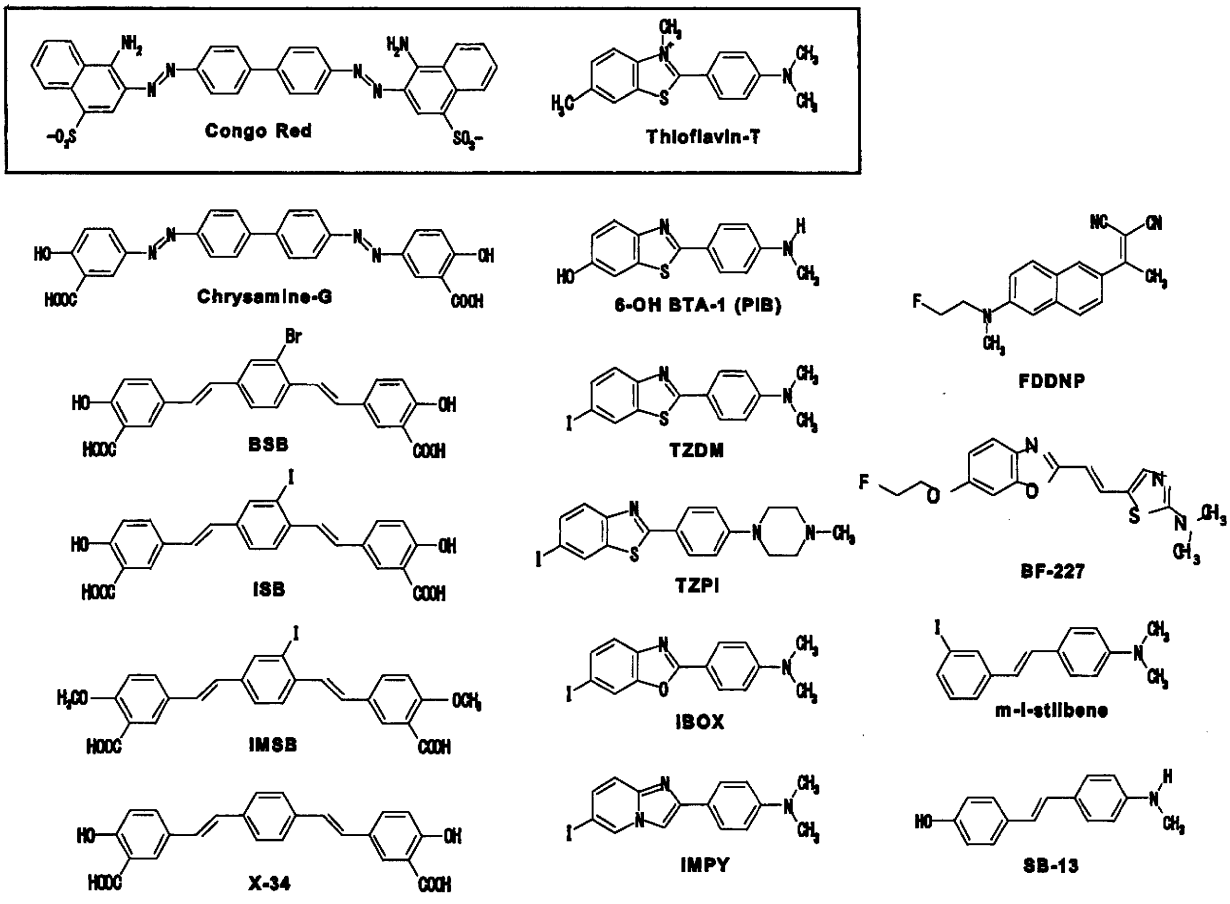

Fig. (2). Chemical structures of common imaging probes for amyloid plaques.

imaging agent and has been used in humans. Other iodinated agents are also under evaluation.

Benzoxazole derivatives are other possible amyloid-imaging agents [20-23]. Their chemical structures, binding affinities for Aβ fibrils, and pharmacokinetic data are summarized in Table 1. Most of these compounds show high binding affinity for both Aβ1-40 and Aβ1-42 fibrils. BF-191 and BF-208, which have halogens as substituents for amino groups, show low affinity for both Aβ1-40 and Aβ1-42 fibrils, suggesting that amino groups have a crucial role in binding to Aβ fibrils. All compounds have good BBB permeability. BF-227 shows faster washout from normal brain tissue than the other compounds [23, 24]. BF-227 distinctly stained SPs during the neuropathological staining of AD brain sections, and this staining pattern correlated well with Aβ immunostaining (Fig. (3)). Fluorescence microscopy revealed that this agent binds preferentially to SPs rather than NFTs. An acute and subacute toxicity study of BF-227 indicated sufficient safety for clinical use as a PET probe.

HUMAN PET STUDY

Human amyloid imaging was first studied using [^{18}F] FDDNP [9]. A [^{18}F]FDDNP PET study revealed regional accumulation of [^{18}F]FDDNP in the SP- and NFT-rich areas of the brain [25]. Global FDDNP-PET binding distinctly differentiated AD patients from normal subjects. FDDNP retention in the medial temporal lobes of subjects with mild cognitive impairment (MCI) was intermediate between levels in AD patients and normal control subjects. This finding is consistent with the observation in an autopsy study that the concentration of NFTs in the medial temporal lobes was intermediate between that in normally aging subjects and AD patients [26]. These binding characteristics indicate that this imaging agent is useful in tracing the progression of AD from the MCI stage. In addition, this agent has the potential to differentiate atypical prion disease from AD [27]. The weakness of this agent is the low signal-to-background ratio of the images, which is due to the considerable amount of nonspecific accumulation in normal brain tissue [28].

In comparison with [^{18}F]FDDNP, [^{11}C]PIB PET images differentiated AD patients from normal individuals more distinctly [29]. PIB retention was observed in the SP-rich neocortex of the brain but not in the NFT-rich medial temporal cortex, indicating that this agent binds selectively to SPs. A quantitative imaging method using PIB has already been validated [30, 31]. Over half the subjects with MCI also showed neocortical PIB accumulation to the same level as AD patients [32, 33]. Interestingly, MCI subjects who at clinical follow-up converted to AD showed higher PIB retention than subjects with non-progressive MCI, indicating that neocortical PIB retention is a marker for the prediction of progression to AD in the MCI stage [34]. A PIB-PET study in a nondemented population revealed elevated cortical retention of PIB in four nondemented persons [35]. These nondemented PIB-positive cases additionally showed an abnormality in the concentration of Aβ1-42 in cerebrospinal fluid, suggesting the presence of SPs in the absence of cognitive impairment [36]. There was a strong relationship between impaired memory performance and PIB binding in the nondemented population [37]. These findings suggest that amyloid imaging may be sensitive enough for the detection of a preclinical AD state. However, one should be careful when assessing abnormalities in the distribution of PIB, because PIB retention is also observed in cerebral amyloid angiopathy [38, 39]. Amyloid imaging may be useful as a surrogate marker for monitoring brain amyloid deposition during anti-amyloid therapy. However, longitudinal PIB-PET evaluation indicated relatively stable PIB retention after 2 years of follow-up in AD patients, suggesting that brain amyloid deposition reflected by PIB retention reaches a plateau at the early clinical stages of AD [40]. Therefore, therapy that retards the synthesis of Aβ (e.g., β- and γ-secretase inhibitors) should be started before the retention of amyloid-imaging tracers reaches a plateau.

The stilbene derivative SB-13 has also been used in a human PET study [41]. In a PET study, [^{11}C]SB-13 exhibited similar binding properties to PIB. For expanded use in clinical investigations, an ^{18}F-labeled stilbene derivative is under investigation.

A PET study using [^{11}C]BF-227 was performed at Tohoku University [23]. Neocortical retention of BF-227 was observed in an AD patient (Fig. (4)). A subject with MCI also showed cortical retention of BF-227. Interestingly, this subject was confirmed to progress to AD during the follow-up period, suggesting that cortical retention of BF-227 indicates a high risk of conversion to AD in MCI subjects. Several MCI subjects showed a distribution of BF-227 similar to that in normally aged subjects. All Alzheimer's patients and about 60% of MCI subjects showed an elevated standardized uptake value (SUV) ratio in the neocortical regions. Even in MCI subjects showing prominent retention of BF-227, the neocortical SUV ratio was below the mean value observed in AD patients. This finding suggests that MCI is a pathologically transitional state between normal aging and dementia, and that the amyloid deposition reflected by BF-227 retention does not reach a plateau in the MCI stage. Voxel-by-voxel analysis of BF-227 PET images demonstrated higher retention of BF-227 in the temporoparietal region in AD patients [23]. The pattern of distribution resembles the distribution of neuritic plaques in postmortem AD brains [42, 43]. Microscopic observation also indicates preferential binding of BF-227 to neuritic plaques in AD brain sections (Fig. (3)). In an *in vitro* binding experiment, BF-227 binding to Aβ increased linearly with increasing Aβ fibril formation [24]. For these reasons, BF-227 is considered to bind neuritic plaques selectively *in vivo*. A validation study is required to determine whether the retention of BF-227 in the neocortex accurately reflects the level of neuritic plaques rather than the level of diffuse plaques.

FUTURE DIRECTION OF PROBE DEVELOPMENT

The commercialization of ^{18}F-labeled agents or SPECT imaging agents is necessary for the wide clinical application of amyloid imaging. Because of the limited half-life of ^{11}C (20 min), the supply of ^{11}C-labeled PET agents is limited to facilities with an on-site cyclotron. ^{18}F-labeled agents are generally easier for routine clinical use because of the longer half-life of ^{18}F (110 min). Currently, several ^{18}F-labeled agents for amyloid imaging are under clinical evaluation. To

Table 1. Binding Affinity of Benzoxazole Derivatives for Aβ Fibrils and Brain Uptakes After Intravenous Administration in Normal Mice

Compounds	Chemical structure	Kd or Ki (nM)		Brain uptake (%ID/g)	
		Aβ1-40	Aβ1-42	2 min	30 min
BF-125	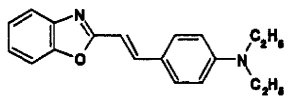	1.5 ± 0.76	4.9 ± 1.9	3.0 ± 0.87	3.0 ± 0.53
BF-133	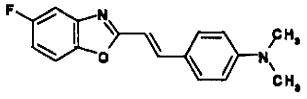	2.1 ± 1.1	3.4 ± 0.73	5.5 ± 0.40	3.8 ± 0.030
BF-140	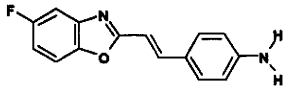	4.7 ± 2.2	2.1 ± 0.18	5.5 ± 0.60	1.1 ± 0.076
BF-145	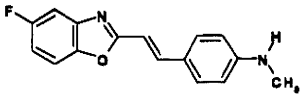	3.0 ± 0.46	4.5 ± 1.9	4.4 ± 1.80	1.6 ± 0.40
BF-168	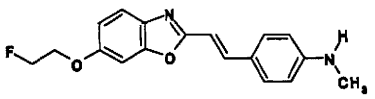	2.5 ± 2.3	6.4 ± 1.0	3.9 ± 0.22	1.6 ± 0.0071
BF-180	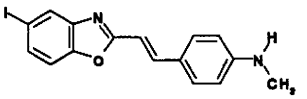	6.8 ± 1.4	10.6 ± 1.5	2.4 ± 0.52	1.8 ± 0.010
BF-185	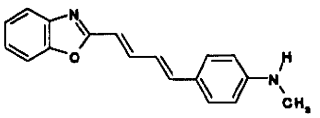	2.5 ± 2.3	14 ± 10	3.9 ± 0.49	3.8 ± 0.16
BF-191	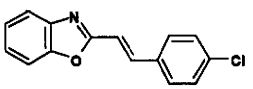	> 5000	> 5000	12 ± 0.26	1.7 ± 0.16
BF-208	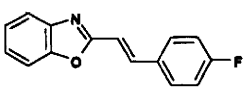	> 5000	> 5000	5.6 ± 0.64	0.28 ± 0.024
BF-227	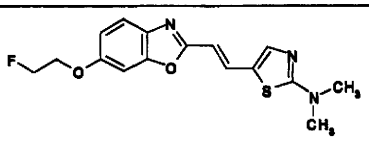	1.8 ± 0.42	4.3 ± 1.5	7.9 ± 0.18	0.54 ± 0.029

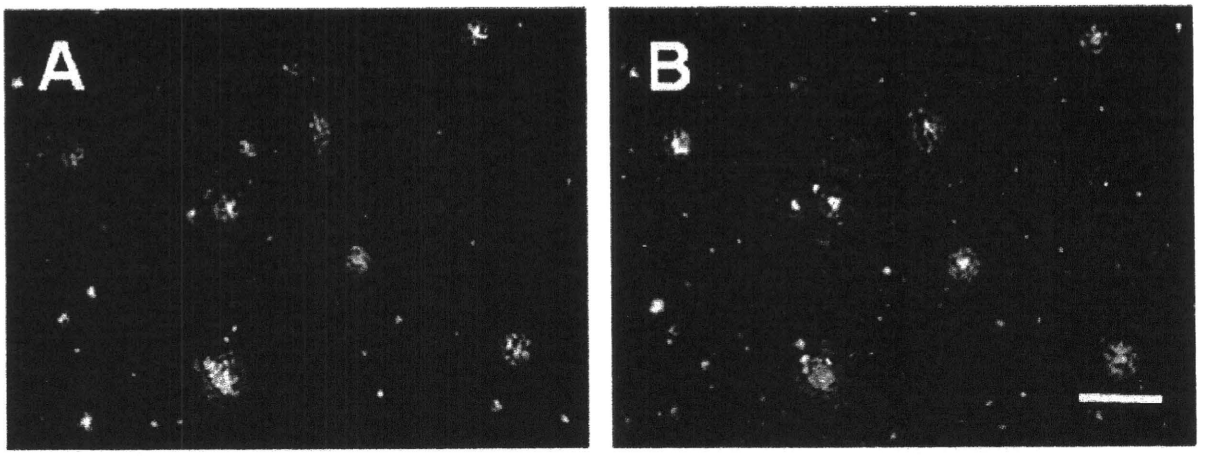

Fig. (3). Fluorescence microscopic images of senile plaques in Alzheimer's disease using BF-227 (A) and Aβ specific antibody 6F/3D (B) Bar = 100μm.

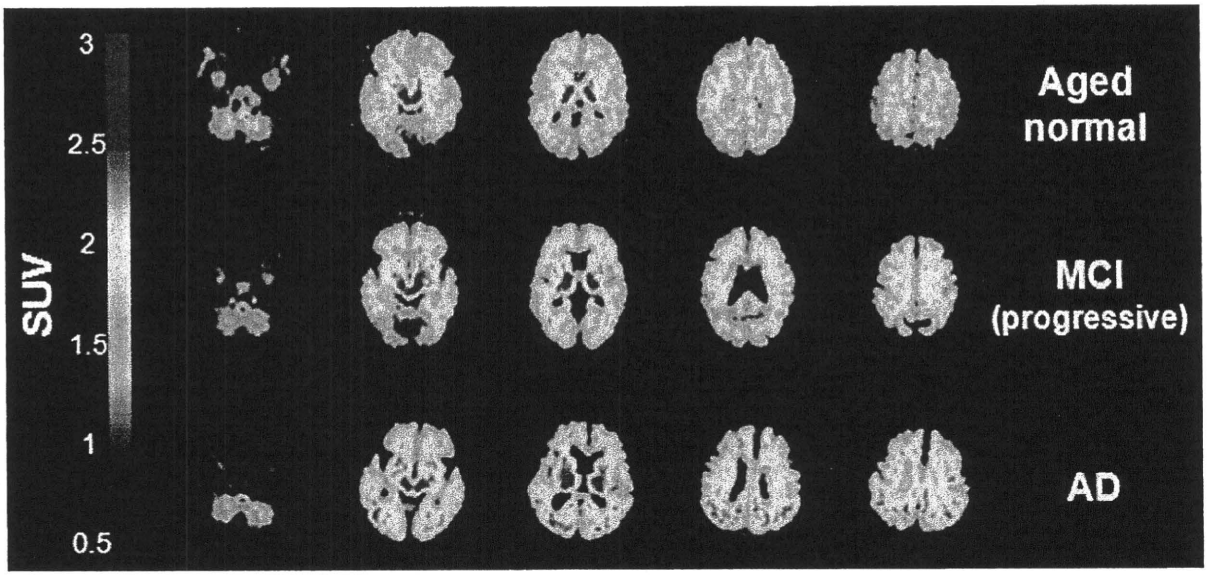

Fig. (4). Mean SUV images between 20 and 40 min post-injection of [^{11}C]BF-227 in aged normal, MCI and AD cases.

obtain a better understanding of the pathophysiology of AD, it is also necessary to visualize the distributions of Aβ pathology and tau pathology individually. However, no surrogate markers are available for evaluating the deposition of NFTs in the brain, because of the difficulty in developing a tau-specific imaging probe [44]. We previously introduced the novel compounds BF-126 and BF-170 as candidates for tau imaging [45]. In AD brain sections, BF-126 and BF-170 visualize NFTs, neuropil threads, and PHF-type neuritis distinctly. For clinical application, optimization of these compounds to reduce non-specific binding is in progress.

CONCLUSION

Several amyloid-imaging agents have been successfully developed for PET imaging. These agents displayed high binding affinity for Aβ fibrils and high BBB permeability. [^{11}C]PIB, [^{18}F]FDDNP, and [^{11}C]BF-227 displayed selective *in vivo* binding to amyloid in the brain and clearly differentiated early AD patients from normal populations. The development of ^{18}F-labeled agents or SPECT imaging agents is necessary for the wide application of amyloid imaging. The development of an NFT-specific imaging agent is also much needed. Amyloid imaging is currently the best method for the early and accurate diagnosis of AD and for monitoring amyloid pathology in the brain. This imaging technology and the forthcoming anti-amyloid therapy will cooperatively contribute to the prevention of dementia.

ACKNOWLEDGEMENTS

This study was partially supported by the Special Coordination Funds for Promoting Science and Technology, the Program for the Promotion of Fundamental Studies in Health Science of the National Institute of Biomedical Innovation, the Industrial Technology Research Grant

Program of the New Energy and Industrial Technology Development Organization (NEDO) of Japan, Health and Labour Sciences Research Grants for Translational Research from the Japanese Ministry of Health, Labour and Welfare, and a JST grant for research and education in molecular imaging.

DISCLOSURE STATEMENT

All authors have no conflict of interest.

REFERENCES

[1] Tanzi RE, Bertram L. Twenty years of the Alzheimer's disease amyloid hypothesis: a genetic perspective. Cell 2005; 120: 545-555.

[2] Goldman WP, Price JL, Storandt M, *et al.* Absence of cognitive impairment or decline in preclinical Alzheimer's disease. Neurology 2001; 56: 361-367.

[3] Price JL, Morris JC. Tangles and plaques in nondemented aging and "preclinical" Alzheimer's disease. Ann Neurol 1999; 45: 358-368.

[4] Klunk WE, Debnath ML, Pettegrew JW. Development of small molecule probes for the beta-amyloid protein of Alzheimer's disease. Neurobiol Aging 1994; 691-698.

[5] Klunk WE, Debnath ML, Pettegrew JW. Chrysamine-G binding to Alzheimer and control brain: autopsy study of a new amyloid probe. Neurobiol Aging 1995; 16: 541-548.

[6] Skovronsky DM, Zhang B, Kung MP, Kung HF, Trojanowski JQ, Lee VM. *In vivo* detection of amyloid plaques in a mouse model of Alzheimer's disease. Proc Natl Acad Sci USA 2000; 97: 7609-7614.

[7] Zhuang ZP, Kung MP, Hou C, *et al.* Radioiodinated styrylbenzenes and thioflavins as probes for amyloid aggregates. J Med Chem 2001; 44: 1905-1914.

[8] Klunk WE, Bacskai BJ, Mathis CA, *et al.* Imaging Abeta plaques in living transgenic mice with multiphoton microscopy and methoxy-X04, a systemically administered Congo red derivative. J Neuropathol Exp Neurol 2002; 61: 797-805.

[9] Shoghi-Jadid K, Small GW, Agdeppa ED, *et al.* Localization of neurofibrillary tangles and beta-amyloid plaques in the brains of living patients with Alzheimer disease. Am J Geriatr Psychiatry 2002; 10: 24-35.

[10] Agdeppa ED, Kepe V, Liu J, *et al.* Binding characteristics of radiofluorinated 6-dialkylamino-2-naphthylethylidene derivatives as positron emission tomography imaging probes for beta-amyloid plaques in Alzheimer's disease. J Neurosci 2001; 21: RC189.

[11] Agdeppa ED, Kepe V, Petri A, *et al. In vitro* detection of (S)-naproxen and ibuprofen binding to plaques in the Alzheimer's brain using the positron emission tomography molecular imaging probe 2-(1-[6-[(2-[(18)F]fluoroethyl)(methyl) amino]-2-naphthyl]ethylidene)malononitrile. Neuroscience 2003; 117: 723-730.

[12] Mathis CA, Wang Y, Klunk WE. Imaging beta-amyloid plaques and neurofibrillary tangles in the aging human brain. Curr Pharm Des 2004; 10: 1469-1492.

[13] Klunk WE, Wang Y, Huang GF, Debnath ML, Holt DP, Mathis CA. Uncharged thioflavin-T derivatives bind to amyloid-beta protein with high affinity and readily enter the brain. Life Sci 2001; 69: 1471-1484.

[14] Klunk WE, Wang Y, Huang GF, *et al.* The binding of 2-(4'-methylaminophenyl)benzothiazole to postmortem brain homogenates is dominated by the amyloid component. J Neurosci 2003; 23: 2086-2092.

[15] Kung MP, Hou C, Zhuang ZP, *et al.* IMPY: an improved thioflavin-T derivative for *in vivo* labeling of beta-amyloid plaques. Brain Res 2002; 956: 202-210.

[16] Kung HF, Kung MP, Zhuang ZP, *et al.* Iodinated tracers for imaging amyloid plaques in the brain. Mol Imaging Biol 2003; 5: 418-426.

[17] Ono M, Wilson A, Nobrega J, *et al.* ^{11}C-labeled stilbene derivatives as Abeta-aggregate-specific PET imaging agents for Alzheimer's disease. Nucl Med Biol 2003; 30: 565-571.

[18] Ono M, Kawashima H, Nonaka A, *et al.* Novel benzofuran derivatives for PET imaging of beta-amyloid plaques in Alzheimer's disease brains. J Med Chem 2006; 49: 2725-2730.

[19] Suemoto T, Okamura N, Shiomitsu T, *et al. In vivo* labeling of amyloid with BF-108. Neurosci Res 2004; 48: 65-74.

[20] Okamura N, Suemoto T, Shimadzu H, *et al.* Styrylbenzoxazole derivatives for *in vivo* imaging of amyloid plaques in the brain. J Neurosci 2004; 24: 2535-2541.

[21] Okamura N, Suemoto T, Shiomitsu T, *et al.* A novel imaging probe for *in vivo* detection of neuritic and diffuse amyloid plaques in the brain. J Mol Neurosci 2004; 24: 247-255.

[22] Furumoto S, Okamura N, Iwata R, Yanai K, Arai H, Kudo Y. Recent advances in the development of amyloid imaging agents. Curr Top Med Chem 2007; 7: 1773-1789.

[23] Kudo Y, Okamura N, Furumoto S, *et al.* 2-(2-[2-Dimethylaminothiazol-5-yl]ethenyl)-6- (2-[fluoro]ethoxy)benzoxazole: a novel PET agent for *in vivo* detection of dense amyloid plaques in Alzheimer's disease patients. J Nucl Med 2007; 48: 553-561.

[24] Okamura N, Furumoto S, Funaki Y, *et al.* Binding and safety profile of novel benzoxazole derivative for *in vivo* imaging of amyloid deposits in Alzheimer's disease. Geriatr Gerontol Int 2007 (in press)

[25] Small GW, Kepe V, Ercoli LM, *et al.* PET of brain amyloid and tau in mild cognitive impairment. N Engl J Med 2006; 355: 2652-2663.

[26] Petersen RC, Parisi JE, Dickson DW, *et al.* Neuropathologic features of amnestic mild cognitive impairment. Arch Neurol 2006; 63: 665-672.

[27] Boxer AL, Rabinovici GD, Kepe V, *et al.* Amyloid imaging in distinguishing atypical prion disease from Alzheimer disease. Neurology 2007; 69: 283-290.

[28] Bacskai BJ, Klunk WE, Mathis CA, Hyman BT. Imaging amyloid-beta deposits *in vivo*. J Cereb Blood Flow Metab 2002; 22: 1035-1041.

[29] Klunk WE, Engler H, Nordberg A, *et al.* Imaging brain amyloid in Alzheimer's disease with Pittsburgh Compound-B. Ann Neurol 2004; 55: 306-319.

[30] Price JC, Klunk WE, Lopresti BJ, *et al.* Kinetic modeling of amyloid binding in humans using PET imaging and Pittsburgh Compound-B. J Cereb Blood Flow Metab 2005; 25: 1528-1547.

[31] Lopresti BJ, Klunk WE, Mathis CA, *et al.* Simplified quantification of Pittsburgh Compound B amyloid imaging PET studies: a comparative analysis. J Nucl Med 2005; 46: 1959-1972.

[32] Rowe CC, Ng S, Ackermann U, *et al.* Imaging beta-amyloid burden in aging and dementia. Neurology. 2007; 68: 1718-1725.

[33] Kemppainen NM, Aalto S, Wilson IA, *et al.* PET amyloid ligand [^{11}C]PIB uptake is increased in mild cognitive impairment. Neurology 2007; 68: 1603-1606.

[34] Forsberg A, Engler H, Almkvist O, *et al.* PET imaging of amyloid deposition in patients with mild cognitive impairment. Neurobiol Aging 2007 (in press)

[35] Mintun MA, Larossa GN, Sheline YI, *et al.* [^{11}C]PIB in a nondemented population: potential antecedent marker of Alzheimer disease. Neurology 2006; 67: 446-452.

[36] Fagan AM, Mintun MA, Mach RH, *et al.* Inverse relation between *in vivo* amyloid imaging load and cerebrospinal fluid Abeta42 in humans. Ann Neurol 2006; 59: 512-519.

[37] Pike KE, Savage G, Villemagne VL, *et al.* Beta-amyloid imaging and memory in non-demented individuals: evidence for preclinical Alzheimer's disease. Brain 2007; 130: 2837-2844.

[38] Bacskai BJ, Frosch MP, Freeman SH, *et al.* Molecular imaging with Pittsburgh Compound B confirmed at autopsy: a case report. Arch Neurol 2007; 64: 431-434.

[39] Johnson KA, Gregas M, Becker JA, *et al.* Imaging of amyloid burden and distribution in cerebral amyloid angiopathy. Ann Neurol 2007; 62: 229-234.

[40] Engler H, Forsberg A, Almkvist O, *et al.* Two-year follow-up of amyloid deposition in patients with Alzheimer's disease. Brain 2006; 129: 2856-2866.

[41] Verhoeff NP, Wilson AA, Takeshita S, *et al.* In-vivo imaging of Alzheimer disease beta-amyloid with [^{11}C]SB-13 PET. Am J Geriatr Psychiatry 2004; 12: 584-595.

[42] Arnold SE, Hyman BT, Flory J, Damasio AR, Van Hoesen GW. The topographical and neuroanatomical distribution of neurofibrillary tangles and neuritic plaques in the cerebral cortex of patients with Alzheimer's disease. Cereb Cortex 1991; 1: 103-116.

[43] Cummings JL, Cole G. Alzheimer disease. JAMA 2002; 287: 2335-2338.

[44] Small GW, Agdeppa ED, Kepe V, Satyamurthy N, Huang SC, Barrio JR. *In vivo* brain imaging of tangle burden in humans. J Mol Neurosci 2002; 19: 323-327.

[45] Okamura N, Suemoto T, Furumoto S, *et al.* Quinoline and benzimidazole derivatives: candidate probes for *in vivo* imaging of tau pathology in Alzheimer's disease. J Neurosci 2005; 25: 10857-10862.

Received: December 5, 2007 Revised: December 7, 2007 Accepted: December 10, 2007